Chapter 2

High order schemes and their error analysis for generalized variable coefficients fractional reaction-diffusion equations[1]

In this chapter, we examine the following generalized fractional reaction-diffusion problem with variable coefficients, which is more general than that in [66, 67, 119] :

$$ {}_0^C D^{\alpha}_{t:[z(t),\omega(t)]} v(x,t) + q(t)v(x,t) = p(t)\frac{\partial^2 v(x,t)}{\partial x^2} + \mathscr{F}(x,t),\ (x,t) \in (0,b)\times(0,T], \quad (2.1) $$

with initial and boundary conditions

$$ \begin{cases} v(x,0) = g_0(x), & x \in [0,b], \\ v(0,t) = \hat{\phi}_1(t), & t \in (0,T], \\ v(b,t) = \hat{\phi}_2(t), & t \in (0,T], \end{cases} \quad (2.2) $$

where $0 < \alpha < 1$, $q \geq 0$, $p > p_0 \geq 0$, g_0, $\hat{\phi}_1$, $\hat{\phi}_2$ and $\mathscr{F}$ are known sufficiently smooth functions. Moreover, ${}_0^C D^{\alpha}_{t:[z(t),\omega(t)]}$ denotes the generalized fractional differential operator of Caputo type defined in equation (1.19).

Most of the existing works (such as [66, 67, 119] and the references therein) for the present model problem consider the problem without the reaction term and with a

[1]This chapter contains material published in *Mathematical Methods in the Applied Sciences*, 2023, doi: `https://doi.org/10.1002/mma.9458`.

constant $p(t)$. So, it is required to consider a more general problem with variable coefficients. Further, they discretized the space variable using a second order central difference scheme. So, the resulting fully discrete schemes are low-order accurate. Observe that high order numerical methods have great significance because they result in more accurate approximations. So, it is important to develop high order numerical methods for the present problem. Hence, this chapter aims to fill these gaps in the literature.

To smoothen the development and analysis of the methods, we write an equivalent form of (2.1)-(2.2) with the unity weight function $\omega(t)$ and same scale function $z(t)$ by setting $u(x,t) = \omega(t)v(x,t)$:

$$ {}_{0}^{C}D^{\alpha}_{t:[z(t),1]}u(x,t)+q(t)u(x,t) = p(t)\frac{\partial^2 u(x,t)}{\partial x^2}+F(x,t), \quad (x,t) \in (0,b)\times(0,T], \tag{2.3} $$

with initial and boundary conditions

$$ \begin{cases} u(x,0) = g(x), & x \in [0,b], \\ u(0,t) = \phi_1(t), & t \in (0,T], \\ u(b,t) = \phi_2(t), & t \in (0,T], \end{cases} \tag{2.4} $$

where $g(x) = \omega(0)g_0(x)$, $\phi_1(t) = \omega(t)\hat{\phi}_1(t)$, $\phi_2(t) = \omega(t)\hat{\phi}_2(t)$, and $F(x,t) = \omega(t)\mathscr{F}(x,t)$. Once the numerical solution of problem (2.3)-(2.4) is obtained, one can easily compute the numerical solution of problem (2.1)-(2.2) by $u(x,t) = \omega(t)v(x,t)$.

The objectives of this chapter are as follows: To develop and analyze two high-order schemes, $\text{CFD}_{g-\sigma}$ and $\text{PQS}_{g-\sigma}$, for numerically solving problem (2.3)-(2.4). In the $\text{CFD}_{g-\sigma}$ scheme, we consider a fourth order compact difference operator to discretize the spatial derivative and $(3-\alpha)$th order Generalized Alikhanov's formula $(gL2-1_\sigma)$ to approximate the generalized time-fractional derivative of Caputo type, while in the $\text{PQS}_{g-\sigma}$ scheme, we consider a parametric quintic spline scheme to discretize the spatial derivative and $(3-\alpha)$th order Generalized Alikhanov's formula $(gL2-1_\sigma)$ to approximate the generalized time-fractional derivative. Furthermore, for the developed schemes, we thoroughly discuss the stability and convergence analysis and show that the theoretical bounds for the $\text{CFD}_{g-\sigma}$ scheme and $\text{PQS}_{g-\sigma}$ scheme are $\mathcal{O}(\Delta t^{3-\alpha}, \widetilde{\Delta} t^2, h^4)$ and $\mathcal{O}(\Delta t^{3-\alpha}, \widetilde{\Delta} t^2, h^{4.5})$, respectively, where Δt and h represent mesh spacing in time and space directions, respectively.

The arrangement of this chapter is as follows. In Section 2.1, we develop two high-order fully discrete numerical schemes for solving the generalized fractional reaction-diffusion problem. Stability and convergence of both the schemes in $\mathcal{L}_2$- norm have been established separately in Section 2.2. Further, the numerical results of the developed numerical schemes are discussed in Section 2.3 with the help of three test problems. Finally, Section 2.4 concludes the chapter.

2.1 Numerical schemes

In this section, first, we will give the approximation of the generalized fractional derivative. Then we obtain two high order fully discrete numerical schemes approximating problem (2.3)-(2.4).

2.1.1 Discretization of generalized fractional derivative

Throughout this work, we suppose that z (the scale function) is a strictly increasing function. Suppose $\mathcal{Z} : t \to z(t)$ is a mapping from $[0, T]$ to $[z(0), z(T)]$. Suppose N_t is a positive integer. We divide the interval $[0, T]$ into N_t subintervals with non-uniform partition $\Omega_t : 0 = t_0 < t_1 < \cdots < t_{N_t} = T$. Now denote $z(t_j) = z_j$ and consider $z_j = z_0 + j\Delta t$ and $t_j = \mathcal{Z}^{-1}(z_0 + j\Delta t)$, where $\Delta t = \frac{z(T)-z(0)}{N_t} = z(t_{j+1}) - z(t_j)$, $0 \leq j \leq N_t - 1$. Furthermore, let $\widetilde{\Delta} t = \max\limits_{0\leq j\leq N_t-1}(t_{j+1} - t_j)$. Now, let $\sigma = 1 - \frac{\alpha}{2}$. Here, it is obvious that $z(t_{j+\sigma}) = z_{j+\sigma} = z_0 + (j+\sigma)\Delta t$ and $t_{j+\sigma} = \mathcal{Z}^{-1}(z_0 + (j+\sigma)\Delta t)$ for $0 \leq j \leq N_t - 1$. Then, generalized Alikhanov's formula $(gL2 - 1_\sigma)$ for generalized fractional derivative of Caputo type of function $f(\mathcal{Z}^{-1}(z)) \in C^3[z(0), z(T)]$ at $t_{j+\sigma}$ is given by [67]

$$
{}_0^C D^{\alpha}_{t:[z(t),1]} f(t_{j+\sigma}) = \nu \left[w_0 f(t_{j+1}) - \sum_{k=1}^{j} (w_{j-k} - w_{j-k+1}) f(t_k) - w_j f(t_0) \right] + \mathcal{O}(\Delta t^{3-\alpha}), \tag{2.5}
$$

where $\nu = \frac{\Delta t^{-\alpha}}{\Gamma(2-\alpha)}$ and the coefficients w_k's are given as: $w_0 = a_0$, if $j = 0$, and for $j \geq 1$

$$
w_k = \begin{cases} a_0 + b_1, & k = 0, \\ a_k + b_{k+1} - b_k, & 1 \leq k \leq j-1, \\ a_j - b_j, & k = j, \end{cases} \tag{2.6}
$$

with $a_0 = \sigma^{1-\alpha}$,

$$
a_k = (k+\sigma)^{1-\alpha} - (k+\sigma-1)^{1-\alpha}, \quad k \geq 1, \tag{2.7}
$$

$$
b_k = \frac{1}{2-\alpha}\left[(k+\sigma)^{2-\alpha} - (k+\sigma-1)^{2-\alpha}\right] - \frac{1}{2}\left[(k+\sigma)^{1-\alpha} + (k+\sigma-1)^{1-\alpha}\right], \quad k \geq 1. \tag{2.8}
$$

Lemma 2.1. *[67] The coefficients w_k satisfy*

(a). $\quad w_0 > w_1 > \cdots > w_j > 0, \quad j \geq 1.$

(b). $\quad w_j > \frac{1-\alpha}{2(j+\sigma)^\alpha}, \quad j \geq 0.$

(c). $\quad (2\sigma - 1)w_0 - \sigma w_1 > 0.$

2.1.2 The spatial discretization

In this subsection, we will introduce two high order schemes for the spatial discretization of (2.3)-(2.4). For this end, let N_x be a positive integer and divide the interval $[0, b]$ into N_x subintervals with $\Omega_x : 0 = x_0 < x_1 < \cdots < x_{N_x} = b$. Suppose $x_i = ih$, with the mesh width $h = \frac{b}{N_x}$. Let $u(x,t)$ denote the exact solution of problem (2.3)-(2.4). For $0 \le i \le N_x$ and $0 \le j \le N_t$, we shall use the notation $u_i^j = u(x_i, t_j)$ and $F_i^j = F(x_i, t_j)$. Further, let U_i^j denote the approximation of u_i^j. Now, let $\mathcal{D}_h = \{\vartheta | (\vartheta_0, \vartheta_1, \cdots, \vartheta_{N_x})\}$, and $\mathcal{D}_h^* = \{\vartheta | (\vartheta_0, \vartheta_1, \cdots, \vartheta_{N_x}), \vartheta_0 = \vartheta_{N_x} = 0\}$. So, for any grid function $\vartheta \in \mathcal{D}_h$, let us denote

$$\delta_x \vartheta_{i+\frac{1}{2}} = \frac{1}{h}(\vartheta_{i+1} - \vartheta_i), \quad \delta_x^2 \vartheta_i = \frac{1}{h}\left(\delta_x \vartheta_{i+\frac{1}{2}} - \delta_x \vartheta_{i-\frac{1}{2}}\right),$$
$$\delta_x^3 \vartheta_{i+\frac{1}{2}} = \frac{1}{h}(\delta_x^2 \vartheta_{i+1} - \delta_x^2 \vartheta_i), \quad \delta_x^4 \vartheta_i = \frac{1}{h}\left(\delta_x^3 \vartheta_{i+\frac{1}{2}} - \delta_x^3 \vartheta_{i-\frac{1}{2}}\right).$$

2.1.2.1 CFD$_{g-\sigma}$ scheme

Here, we introduce a high order compact scheme (CFD$_{g-\sigma}$) for the spatial discretization of (2.3)-(2.4). Now for any grid function $\vartheta \in \mathcal{D}_h$, the compact differential operator ($\mathcal{H}_c$) is defined as

$$\mathcal{H}_c \vartheta_i = \begin{cases} \frac{1}{12}\vartheta_{i-1} + \frac{10}{12}\vartheta_i + \frac{1}{12}\vartheta_{i+1}, & 1 \le i \le N_{\mathrm{x}} - 1, \\ \vartheta_i, & i = 0 \text{ or } N_{\mathrm{x}}. \end{cases} \tag{2.9}$$

Also, here it is evident that

$$\mathcal{H}_c \vartheta_i = \left(I + \frac{h^2}{12}\delta_x^2\right)\vartheta_i, \quad 1 \le i \le N_x - 1. \tag{2.10}$$

Lemma 2.2. *[71] Suppose $\psi(x) \in C^6[x_{i-1}, x_{i+1}]$ and $\tilde{\phi}(s) = -3(1-s)^5 + 5(1-s)^3$, then*

$$\frac{1}{12}\psi''(x_{i-1}) + \frac{10}{12}\psi''(x_i) + \frac{1}{12}\psi''(x_{i+1}) = \frac{\psi(x_{i-1}) - 2\psi(x_i) + \psi(x_{i+1})}{h^2} + \frac{h^4}{360}\int_0^1 \left(\psi^{(6)}(x_i - sh) + \psi^{(6)}(x_i + sh)\right)\tilde{\phi}(s)ds.$$

Now consider problem (2.3) at $(x_i, t_{j+\sigma})$, $0 \le i \le N_x, 0 \le j \le N_t - 1$. We have

$${}_0^C D^{\alpha}_{t:[z(t),1]} u(x_i, t_{j+\sigma}) + q(t_{j+\sigma})u(x_i, t_{j+\sigma}) = p(t_{j+\sigma})\frac{\partial^2 u(x_i, t_{j+\sigma})}{\partial x^2} + F(x_i, t_{j+\sigma}). \quad (2.11)$$

Lemma 2.3. *[67] If $W(t) \in C^2[0, T]$, then on the non-uniform mesh Ω_t, we have*

$$W(t_{j+\sigma_j}) \equiv \sigma_j W(t_{j+1}) + (1-\sigma_j)W(t_j) = W(t_{j+\sigma}) + \mathcal{O}(\widetilde{\Delta} t^2),$$

where $\sigma = 1 - \frac{\alpha}{2}$, $\sigma_j = \frac{t_{j+\sigma} - t_j}{t_{j+1} - t_j} \in (0, 1)$, and $\widetilde{\Delta} t = \max\limits_{0 \le j \le N_t - 1}(t_{j+1} - t_j)$.

Now in order to derive the CFD$_{g-\sigma}$ scheme, we use the $gL2-1_\sigma$ approximation of generalized fractional derivative given in equation (2.5) and apply the compact operator $\mathcal{H}_c$ defined in equation (2.9) to both sides of equation (2.11). Further, we approximate $u_i^{j+\sigma}$ (and similarly $u_{i-1}^{j+\sigma}$, $u_{i+1}^{j+\sigma}$) by Lemma 2.3. We obtain

$$\nu\mathcal{H}_c\left[w_0 u_i^{j+1} - \sum_{k=1}^{j}(w_{j-k} - w_{j-k+1})u_i^k - w_j u_i^0\right] + q^{j+\sigma}\mathcal{H}_c u_i^{j+\sigma_j} = p^{j+\sigma}\delta_x^2 u_i^{j+\sigma_j} + \mathcal{H}_c F_i^{j+\sigma} + {}_cR_i^{j+\sigma}, \ 1 \le i \le N_x - 1, \quad (2.12)$$

$$u_i^0 = g(x_i), \quad 0 \le i \le N_x, \quad (2.13)$$

$$u_0^j = \phi_1(t_j), \quad u_{N_x}^j = \phi_2(t_j), \quad 1 \le j \le N_t, \quad (2.14)$$

where $q^{j+\sigma} = q(t_{j+\sigma})$ and $p^{j+\sigma} = p(t_{j+\sigma})$. Further, removing the truncation error term ${}_cR_i^{j+\sigma} = O(\Delta t^{3-\alpha}, \widetilde{\Delta} t^2, h^4)$ from equation (2.12), we have

$$\nu \mathcal{H}_c \left[w_0 U_i^{j+1} - \sum_{k=1}^{j} (w_{j-k} - w_{j-k+1}) U_i^k - w_j U_i^0 \right] + q^{j+\sigma} \mathcal{H}_c U_i^{j+\sigma_j} = p^{j+\sigma} \delta_x^2 U_i^{j+\sigma_j}, \\ + \mathcal{H}_c F_i^{j+\sigma}, \; 1 \leq i \leq N_x - 1, \tag{2.15}$$

$$U_i^0 = g(x_i), \quad 0 \leq i \leq N_x, \tag{2.16}$$

$$U_0^j = \phi_1(t_j), \quad U_{N_x}^j = \phi_2(t_j), \quad 1 \leq j \leq N_t. \tag{2.17}$$

Thus, we can recursively solve the discrete scheme (2.15)-(2.17) for U_i^j, $1 \leq i \leq N_x - 1$, $1 \leq j \leq N_t$ and obtain the numerical solution of problem (2.3)-(2.4).

2.1.2.2 PQS$_{g-\sigma}$ scheme

Here, we introduce a high order parametric quintic spline operator $\mathcal{H}_q$, which plays a vital role in obtaining the high order spatial discretized scheme for (2.3)-(2.4).

Definition 2.1. [50–52] A function $\mathcal{P}_{\Omega_x}(x;\varsigma) \in C^4[0,b]$, for a given mesh Ω_x is said to be the parametric quintic spline with parameter $\varsigma > 0$ if its restriction $\mathcal{P}_{\Omega_x,i}(x;\varsigma) = \{\mathcal{P}_{\Omega_x}(x;\varsigma)\}_{[x_{i-1},x_i]}$, $1 \leq i \leq N_x$ fulfills the condition $\mathcal{P}_{\Omega_x,i}(x_l) = \vartheta_l$, $l = i-1, i$ and

$$\mathcal{P}^{(4)}_{\Omega_x,i}(x) + \varsigma^2 \mathcal{P}''_{\Omega_x,i}(x) = (\mathcal{F}_i + \varsigma^2 \tilde{\omega}_i) \frac{(x - x_{i-1})}{h} + (\mathcal{F}_{i-1} + \varsigma^2 \tilde{\omega}_{i-1}) \frac{(x_i - x)}{h}, \tag{2.18}$$

where $\mathcal{P}''_{\Omega_x,i}(x_l) = \tilde{\omega}_l$ and $\mathcal{P}^{(4)}_{\Omega_x,i}(x_l) = \mathcal{F}_l$, $l = i-1, i$.

Solving equation (2.18) for $\mathcal{P}_{\Omega_x,i}$ yields

$$\mathcal{P}_{\Omega_x,i}(x) = \rho \vartheta_i + \bar{\rho} \vartheta_{i-1} + \frac{h^2}{6} \left(\chi_1(\rho) \tilde{\omega}_i + \chi_1(\bar{\rho}) \tilde{\omega}_{i-1} \right) + \left(\frac{h}{\tilde{\gamma}} \right)^4 \left(\frac{\tilde{\gamma}^2}{6} \chi_1(\rho) - \chi_2(\rho) \right) \mathcal{F}_i$$

$$+\left(\frac{h}{\tilde{\gamma}}\right)^4\left(\frac{\tilde{\gamma}^2}{6}\chi_1(\bar{\rho})-\chi_2(\bar{\rho})\right)\mathcal{F}_{i-1}, \tag{2.19}$$

where $\tilde{\gamma}=\varsigma h$, $\rho=\frac{(x-x_{i-1})}{h}$, $\bar{\rho}=1-\rho$, $\chi_1(\rho)=\rho^3-\rho$, and $\chi_2(\rho)=\rho-\frac{\sin\tilde{\gamma}\rho}{\sin\tilde{\gamma}}$.

Now using the continuity conditions of the first and third derivatives of $\mathcal{P}_{\Omega_x}(x)$ at $x=x_i$, viz $\mathcal{P}'_{\Omega_x,i}(x_i)=\mathcal{P}'_{\Omega_x,i+1}(x_i)$ and $\mathcal{P}'''_{\Omega_x,i}(x_i)=\mathcal{P}'''_{\Omega_x,i+1}(x_i)$, we have two relations including ϑ_l, $\tilde{\omega}_l$ and $\mathcal{F}_l$, $l=i-1,i,i+1$. After the elimination of $\mathcal{F}_l$, we get

$$\widetilde{p}\tilde{\omega}_{i-2}+\widetilde{q}\tilde{\omega}_{i-1}+\widetilde{s}\tilde{\omega}_i+\widetilde{q}\tilde{\omega}_{i+1}+\widetilde{p}\tilde{\omega}_{i+2}=(\delta_x^2+\mu h^2\delta_x^4)\vartheta_i,\;\; 2\leq i\leq N_x-2, \tag{2.20}$$

where $\mu=\frac{1}{\tilde{\gamma}^2}\left(\frac{\tilde{\gamma}}{\sin\tilde{\gamma}}-1\right)$ and $\widetilde{p}$, $\widetilde{q}$ and $\widetilde{s}$ such that $2\widetilde{p}+2\widetilde{q}+\widetilde{s}=1$.

We can only consider $\mu\in\left(0,\frac{1}{2}\right)$, due to the consistency relation given in [50, 64]. But, using μ in $\left(0,\frac{1}{2}\right)$ provides various schemes with different accuracy.

Apart from equation (2.20), we require two more equations which can be obtained from the following formulation

$$-\mathcal{R}_i=\frac{d_{i-1}\vartheta_{i-1}+d_i\vartheta_i+d_{i+1}\vartheta_{i+1}}{h^2}+d^*_{i-1}\tilde{\omega}_{i-1}+d^*_i\tilde{\omega}_i+d^*_{i+1}\tilde{\omega}_{i+1},\;\; i=1,N_x-1.$$

Here, $\mathcal{R}_i$ denotes the local truncation error at $x=x_i$. d's and d^*'s are the unknown coefficients which are required to be evaluated in such a way that $\mathcal{R}_i=\mathcal{O}(h^4)$ for $i=1,N_x-1$.

Now in the above two equations at $x=x_i$ we carry out the Taylor expansions and taking $\mathcal{R}_i=\mathcal{O}(h^4)$ for $i=1,N_x-1$ provides

$$\left(d_{i-1},d_i,d_{i+1},d^*_{i-1},d^*_i,d^*_{i+1}\right)=\left(-1,2,-1,\frac{1}{12},\frac{10}{12},\frac{1}{12}\right)\;\; i=1,N_x-1.$$

Next, removing the local truncation error term $\mathcal{R}_i$, we get two equations as follows

$$\left(I + \frac{h^2}{12}\delta_x^2\right)\tilde{\omega}_i = \delta_x^2\vartheta_i, \quad i = 1, N_x - 1. \tag{2.21}$$

Thus, combining the equations (2.20) and (2.21), we define the parametric quintic spline operator $\mathcal{H}_q$ as follows

$$\mathcal{H}_q\vartheta_i = \begin{cases} \left(I + \frac{h^2}{12}\delta_x^2\right)\vartheta_i, & i = 1, N_x - 1, \\ \widetilde{p}\vartheta_{i-2} + \widetilde{q}\vartheta_{i-1} + \widetilde{s}\vartheta_i + \widetilde{q}\vartheta_{i+1} + \widetilde{p}\vartheta_{i+2}, & 2 \le i \le N_x - 2. \end{cases} \tag{2.22}$$

Also, for $\mu \in \left(0, \frac{1}{2}\right)$, we introduce the notation

$$\tilde{\delta}_x^2\vartheta_i = \begin{cases} \delta_x^2\vartheta_i, & i = 1, N_x - 1, \\ \left(\delta_x^2 + \mu h^2\delta_x^4\right)\vartheta_i, & 2 \le i \le N_x - 2. \end{cases} \tag{2.23}$$

Now we use Taylor expansions at $x = x_i$ and get the following result.

Lemma 2.4. *Suppose $\vartheta \in C^8[0, b]$. If*

$$\widetilde{p} = \frac{\mu}{12} - \frac{1}{240}, \quad \widetilde{q} = \frac{8\mu}{12} + \frac{1}{10}, \quad \widetilde{s} = -\frac{3\mu}{2} + \frac{97}{120}, \tag{2.24}$$

then the following result holds

$$\mathcal{H}_q\left.\frac{\partial^2\vartheta}{\partial x^2}\right|_{x_i} - \tilde{\delta}_x^2\vartheta_i = \begin{cases} -\frac{h^4}{240}\left.\frac{\partial^6\vartheta}{\partial x^6}\right|_{x_i} + \mathcal{O}(h^6), & i = 1, N_x - 1, \\ \mathcal{Q}h^6\left.\frac{\partial^8\vartheta}{\partial x^8}\right|_{x_i} + \mathcal{O}(h^8), & 2 \le i \le N_x - 2, \end{cases} \tag{2.25}$$

where $\mathcal{Q} = -\frac{8\widetilde{p}}{45} - \frac{\widetilde{q}}{360} + \frac{126\mu}{10080} + \frac{1}{20160}$ *and* $\mu \in \left(0, \frac{1}{2}\right)$.

Remark 2.1. We fix the values of $\widetilde{p}$, $\widetilde{q}$, and $\widetilde{s}$ as given in equation (2.24) for the rest of the chapter.

Now we consider problem (2.3) at $(x_i, t_{j+\sigma})$, $0 \leq i \leq N_x, 0 \leq j \leq N_t - 1$. We have

$$ {}_0^C D^{\alpha}_{t:[z(t),1]} u(x_i, t_{j+\sigma}) + q(t_{j+\sigma}) u(x_i, t_{j+\sigma}) = p(t_{j+\sigma}) \frac{\partial^2 u(x_i, t_{j+\sigma})}{\partial x^2} + F(x_i, t_{j+\sigma}). \quad (2.26) $$

The PQS$_{g-\sigma}$ scheme is obtained using the $gL2-1_\sigma$ approximation of generalized fractional derivative of Caputo type given in equation (2.5), parametric quintic spline operator $\mathcal{H}_q$ defined in equation (2.22), and Lemma 2.3 into equation (2.26). We obtain

$$ \nu \mathcal{H}_q \left[w_0 u_i^{j+1} - \sum_{k=1}^{j} (w_{j-k} - w_{j-k+1}) u_i^k - w_j u_i^0 \right] + q^{j+\sigma} \mathcal{H}_q u_i^{j+\sigma_j} = p^{j+\sigma} \tilde{\delta}_x^2 u_i^{j+\sigma_j} $$
$$ + \mathcal{H}_q F_i^{j+\sigma} + {}_q R_i^{j+\sigma}, \ 1 \leq i \leq N_x - 1, \quad (2.27) $$
$$ u_i^0 = g(x_i), \quad 0 \leq i \leq N_x, \quad (2.28) $$
$$ u_0^j = \phi_1(t_j), \quad u_{N_x}^j = \phi_2(t_j), \quad 1 \leq j \leq N_t, \quad (2.29) $$

where $q^{j+\sigma} = q(t_{j+\sigma})$ and $p^{j+\sigma} = p(t_{j+\sigma})$. Further, in view of equation (2.27), removing the truncation error term ${}_q R_i^{j+\sigma}$, we have

$$ \nu \mathcal{H}_q \left[w_0 U_i^{j+1} - \sum_{k=1}^{j} (w_{j-k} - w_{j-k+1}) U_i^k - w_j U_i^0 \right] + q^{j+\sigma} \mathcal{H}_q U_i^{j+\sigma_j} = p^{j+\sigma} \tilde{\delta}_x^2 U_i^{j+\sigma_j} $$
$$ + \mathcal{H}_q F_i^{j+\sigma}, \ 1 \leq i \leq N_x - 1, \quad (2.30) $$
$$ U_i^0 = g(x_i), \quad 0 \leq i \leq N_x, \quad (2.31) $$
$$ U_0^j = \phi_1(t_j), \quad U_{N_x}^j = \phi_2(t_j), \quad 1 \leq j \leq N_t. \quad (2.32) $$

Thus, we can recursively solve the scheme (2.30)-(2.32) for U_i^j, $1 \leq i \leq N_x - 1$, $1 \leq j \leq N_t$, and obtain the numerical solution of problem (2.3)-(2.4).

2.2 Stability and convergence analysis

In this section, we provide stability and convergence analysis of both schemes: $\mathrm{CFD}_{g-\sigma}$ and $\mathrm{PQS}_{g-\sigma}$. So, first, we define some notation and give a few lemmas which will be useful for the analysis of both schemes.

For any $\bar{u}$, $\bar{v} \in \mathcal{D}_h^*$, we define the discrete inner product, $\mathcal{L}_2$ norm, H^1 semi-norm, and $\mathcal{L}_\infty$ norm as follows

$$< \bar{u}, \bar{v} >= h \sum_{i=1}^{N_x-1} \bar{u}_i \cdot \bar{v}_i, \qquad \|\bar{u}\| = \sqrt{< \bar{u}, \bar{u} >},$$

$$\|\delta_x \bar{u}\| = \sqrt{h \sum_{i=1}^{N_x} \left(\delta_x \bar{u}_{i-\frac{1}{2}}\right)^2}, \quad \|\bar{u}\|_\infty = \max_{1 \le i \le N_x-1} |\bar{u}_i|.$$

Similarly, we can define $\|\delta_x^2 \bar{u}\|$, $\|\mathcal{H}_c \bar{u}\|$, and $\|\mathcal{H}_q \bar{u}\|$.

Lemma 2.5. *[67] For the numbers $\tilde{r}_m$, $0 \le m \le j+1$, the following inequalities hold:*

$$\tilde{r}_{j+1} \sum_{k=0}^{j} (\tilde{r}_{k+1} - \tilde{r}_k) w_{j-k} \ge \frac{1}{2} \sum_{k=0}^{j} \left((\tilde{r}_{k+1})^2 - (\tilde{r}_k)^2\right) w_{j-k} + \frac{1}{2w_0} \left(\sum_{k=0}^{j} (\tilde{r}_{k+1} - \tilde{r}_k) w_{j-k}\right)^2,$$

$$r_j \sum_{k=0}^{j} (\tilde{r}_{k+1} - \tilde{r}_k) w_{j-k} \ge \frac{1}{2} \sum_{k=0}^{j} \left((\tilde{r}_{k+1})^2 - (\tilde{r}_k)^2\right) w_{j-k} - \frac{1}{2(w_0 - w_1)} \left(\sum_{k=0}^{j} (\tilde{r}_{k+1} - \tilde{r}_k) w_{j-k}\right)^2.$$

Lemma 2.6. *[67] If the inverse of the scale function z is concave, then for the numbers $\tilde{r}_m$, $0 \le m \le j+1$, the following inequality hold:*

$$\{\sigma_j \tilde{r}_{j+1} + (1-\sigma_j) \tilde{r}_j\} \sum_{k=0}^{j} (\tilde{r}_{k+1} - \tilde{r}_k) w_{j-k} \ge \frac{1}{2} \sum_{k=0}^{j} \left((\tilde{r}_{k+1})^2 - (\tilde{r}_k)^2\right) w_{j-k},$$

where $\sigma_j = \frac{t_{j+\sigma} - t_j}{t_{j+1} - t_j} \in (0, 1)$.

2.2.1 Stability and convergence analysis of CFD$_{g-\sigma}$ scheme

In this subsection, we provide stability and convergence analysis of the CFD$_{g-\sigma}$ scheme (2.15)-(2.17).

Let $\tilde{u}_i^j$ solve the following problem

$$\nu \mathcal{H}_c \left[w_0 \tilde{u}_i^{j+1} - \sum_{k=1}^{j} (w_{j-k} - w_{j-k+1}) \tilde{u}_i^k - w_j \tilde{u}_i^0 \right] + q^{j+\sigma} \mathcal{H}_c \tilde{u}_i^{j+\sigma_j} = p^{j+\sigma} \delta_x^2 \tilde{u}_i^{j+\sigma_j} + \mathcal{H}_c \hat{F}_i^{j+\sigma}, \ 1 \le i \le N_x - 1, \tag{2.33}$$

$$\tilde{u}_i^0 = \hat{g}(x_i), \quad 0 \le i \le N_x, \tag{2.34}$$

$$\tilde{u}_0^j = \phi_1(t_j), \quad \tilde{u}_{N_x}^j = \phi_2(t_j), \quad 1 \le j \le N_t. \tag{2.35}$$

Suppose $e_i^j = \tilde{u}_i^j - U_i^j$. Then, from equations (2.15)-(2.17) and (2.33)-(2.35), it is evident that $e_i^j \in \mathcal{D}_h^*$ and solves the following linear system

$$\nu \mathcal{H}_c \left[w_0 e_i^{j+1} - \sum_{k=1}^{j} (w_{j-k} - w_{j-k+1}) e_i^k - w_j e_i^0 \right] + q^{j+\sigma} \mathcal{H}_c e_i^{j+\sigma_j} = p^{j+\sigma} \delta_x^2 e_i^{j+\sigma_j} + \mathcal{H}_c \tilde{F}_i^{j+\sigma}, \ 1 \le i \le N_x - 1, \tag{2.36}$$

$$e_i^0 = \hat{g}(x_i) - g(x_i), \quad 0 \le i \le N_x, \tag{2.37}$$

$$e_0^j = 0, \quad e_{N_x}^j = 0, \quad 1 \le j \le N_t, \tag{2.38}$$

where $\tilde{F}_i^{j+\sigma} = \hat{F}_i^{j+\sigma} - F_i^{j+\sigma}$. Now we will prove a result that will directly show the stability of CFD$_{g-\sigma}$ scheme (2.15)-(2.17).

Theorem 2.1. *Suppose the inverse of the scale function z is concave. Then the solution to the discrete problem (2.36)-(2.38) satisfies*

$$\|e^{j+1}\|^2 \le \frac{12}{5} \left[\|\mathcal{H}_c e^0\|^2 + c \max_{0 \le l \le N_t - 1} \|\mathcal{H}_c \tilde{F}^{l+\sigma}\|^2 \right], \tag{2.39}$$

where $c = \frac{(z(T)-z(0))^{\alpha}\Gamma(1-\alpha)}{\epsilon}$ *and* $\epsilon = \frac{8p^{j+\sigma}}{3b} > 0$.

Proof. Multiplying equation (2.36) with $h\mathcal{H}_c e_i^{j+\sigma_j}$ and then summing from $i = 1$ to $N_x - 1$, we get

$$\nu\left[w_0(\mathcal{H}_c e^{j+\sigma_j}, \mathcal{H}_c e^{j+1}) - \sum_{k=1}^{j}(w_{j-k} - w_{j-k+1})(\mathcal{H}_c e^{j+\sigma_j}, \mathcal{H}_c e^{k}) - w_j(\mathcal{H}_c e^{j+\sigma_j}, \mathcal{H}_c e^{0})\right]$$
$$= p^{j+\sigma}(\mathcal{H}_c e^{j+\sigma_j}, \delta_x^2 e^{j+\sigma_j}) - q^{j+\sigma}(\mathcal{H}_c e^{j+\sigma_j}, \mathcal{H}_c e^{j+\sigma_j}) + (\mathcal{H}_c e^{j+\sigma_j}, \mathcal{H}_c \hat{F}^{j+\sigma}). \quad (2.40)$$

Now applying Lemma 2.6 to the left side of the equation gives

$$w_0(\mathcal{H}_c e^{j+\sigma_j}, \mathcal{H}_c e^{j+1}) - \sum_{k=1}^{j}(w_{j-k} - w_{j-k+1})(\mathcal{H}_c e^{j+\sigma_j}, \mathcal{H}_c e^{k}) - w_j(\mathcal{H}_c e^{j+\sigma_j}, \mathcal{H}_c e^{0})$$
$$\geq \frac{1}{2}\left[w_0\|\mathcal{H}_c e^{j+1}\|^2 - \sum_{k=1}^{j}(w_{j-k} - w_{j-k+1})\|\mathcal{H}_c e^{k}\|^2 - w_j\|\mathcal{H}_c e^{0}\|^2\right]. \quad (2.41)$$

Next,

$$\begin{aligned}
(\mathcal{H}_c e^{j+\sigma_j}, \delta_x^2 e^{j+\sigma_j}) &= (e^{j+\sigma_j}, \delta_x^2 e^{j+\sigma_j}) + \frac{h^2}{12}(\delta_x^2 e^{j+\sigma_j}, \delta_x^2 e^{j+\sigma_j}) \\
&\leq -h\sum_{i=0}^{N_x-1}\left(\delta_x e_{i+\frac{1}{2}}^{j+\sigma_j}\right)^2 + \frac{h}{6}\left[\sum_{i=1}^{N_x-1}\left(\delta_x e_{i+\frac{1}{2}}^{j+\sigma_j}\right)^2 + \sum_{i=1}^{N_x-1}\left(\delta_x e_{i-\frac{1}{2}}^{j+\sigma_j}\right)^2\right], \\
&\quad \left(\text{since } h^2\left(\delta_x^2 e_i^{j+\sigma_j}\right)^2 \leq 2\left(\delta_x e_{i+\frac{1}{2}}^{j+\sigma_j}\right)^2 + 2\left(\delta_x e_{i-\frac{1}{2}}^{j+\sigma_j}\right)^2\right), \\
&\leq -\frac{2}{3}\sum_{i=0}^{N_x-1} h\left(\delta_x e_{i+\frac{1}{2}}^{j+\sigma_j}\right)^2, \quad \text{(using discrete Poincare inequality)}, \\
&\leq -\frac{8}{3b}\|e^{j+\sigma_j}\|^2. \qquad (2.42)
\end{aligned}$$

Moreover, for $\epsilon = \frac{8p^{j+\sigma}}{3b} > 0$, the Young's inequality yields

$$(\mathcal{H}_c e^{j+\sigma_j}, \mathcal{H}_c \hat{F}^{j+\sigma}) \leq \epsilon\|\mathcal{H}_c e^{j+\sigma_j}\|^2 + \frac{1}{4\epsilon}\|\mathcal{H}_c \tilde{F}^{j+\sigma}\|^2$$

$$= h\epsilon \sum_{i=1}^{N_x-1} \left(\frac{e_{i-1}^{j+\sigma_j} + 10e_i^{j+\sigma_j} + e_{i+1}^{j+\sigma_j}}{12} \right)^2 + \frac{1}{4\epsilon} \|\mathcal{H}_c \tilde{F}^{j+\sigma}\|^2$$

$$= \frac{8p^{j+\sigma}}{3b} \|e^{j+\sigma_j}\|^2 + \frac{3b}{32p^{j+\sigma}} \|\mathcal{H}_c \tilde{F}^{j+\sigma}\|^2. \tag{2.43}$$

Now the use of inequalities (2.41), (2.42) and (2.43) in equation (2.40) yields

$$w_0\|\mathcal{H}_c e^{j+1}\|^2 - \sum_{k=1}^{j}(w_{j-k} - w_{j-k+1})\|\mathcal{H}_c e^k\|^2 - w_j\|\mathcal{H}_c e^0\|^2 \leq \frac{3b}{16\nu p^{j+\sigma}} \|\mathcal{H}_c \tilde{F}^{j+\sigma}\|^2,$$

which gives

$$w_0\|\mathcal{H}_c e^{j+1}\|^2 - \sum_{k=1}^{j}(w_{j-k} - w_{j-k+1})\|\mathcal{H}_c e^k\|^2 \leq w_j \left[\|\mathcal{H}_c e^0\|^2 + \frac{3b}{16\nu p^{j+\sigma} w_j} \|\mathcal{H}_c \tilde{F}^{j+\sigma}\|^2 \right].$$

Thus, using Lemma 2.1 and noting that $(j+\sigma)\Delta t = \frac{(j+\sigma)(z(T)-z(0))}{N_t} < (z(T) - z(0))$, we get

$$w_0\|\mathcal{H}_c e^{j+1}\|^2 - \sum_{k=1}^{j}(w_{j-k} - w_{j-k+1})\|\mathcal{H}_c e^k\|^2 \leq w_j \chi, \tag{2.44}$$

where

$$\chi = \|\mathcal{H}_c e^0\|^2 + \frac{\Gamma(1-\alpha)(z(T)-z(0))^\alpha}{\epsilon} \max_{0 \leq l \leq N_t - 1} \|\mathcal{H}_c \tilde{F}^{l+\sigma}\|^2.$$

Now we prove by induction that

$$\|\mathcal{H}_c e^{j+1}\|^2 \leq \chi, \quad 0 \leq j \leq N_t - 1. \tag{2.45}$$

Putting $j = 0$ in equation (2.44) we get

$$\|\mathcal{H}_c e^1\|^2 \leq \chi,$$

which is identical to (2.45) for $j = 0$. Now let us assume that (2.45) holds for $j = 0, 1, \ldots, n-1$, that is

$$\|\mathcal{H}_c e^{j+1}\|^2 \leq \chi, \quad 0 \leq j \leq n-1. \tag{2.46}$$

Now using $j = n$ in inequality (2.44) together with assumption (2.46) we get

$$\begin{aligned} w_0\|\mathcal{H}_c e^{n+1}\|^2 &\leq \sum_{k=1}^{n}(w_{n-k} - w_{n-k+1})\|\mathcal{H}_c e^k\|^2 + w_n\chi \leq \left[\sum_{k=1}^{n}(w_{n-k} - w_{n-k+1}) + w_n\right]\chi \\ &= w_0\chi. \end{aligned}$$

Thus, (2.46) holds for all j. Since the norms $\|\mathcal{H}_c e\|$ and $\|e\|$ are equivalent from the inequalities

$$\frac{5}{12}\|e\| \leq \|\mathcal{H}_c e\| \leq \|e\|. \tag{2.47}$$

Thus, (2.39) follows from (2.45) and the first inequality in (2.47). $\square$

Now we will prove the main convergence theorem.

Theorem 2.2. *Let $u(x,t) \in C^{6,2}([0,b] \times [0,T])$ be the solution of problem (2.3)-(2.4), $u(x, \mathcal{Z}^{-1}(z)) \in C^3[z(T) - z(0)]$ for any fixed x, inverse of z is concave, and $\{U_i^j, 0 \leq i \leq N_x, 1 \leq j \leq N_t\}$ be the solution of the discrete problem (2.15)-(2.17). Then, the following result holds*

$$\|u_i^{j+1} - U_i^{j+1}\| \leq c\ \mathcal{O}(\Delta t^{3-\alpha}, \widetilde{\Delta} t^2, h^4),$$

where $c = \sqrt{\frac{12(z(T)-z(0))^{\alpha}\Gamma(1-\alpha)}{5\epsilon}}$ and $\epsilon = \frac{8p^{j+\sigma}}{3b}$.

Proof. Let $\xi_i^{j+1} = u_i^{j+1} - U_i^{j+1}$. Now subtracting the linear system (2.15)-(2.17) from (2.12)-(2.14), we get

$$\nu\mathcal{H}_c\left[w_0\xi_i^{j+1} - \sum_{k=1}^{j}(w_{j-k} - w_{j-k+1})\xi_i^k - w_j\xi_i^0\right] + q^{j+\sigma}\mathcal{H}_c\xi_i^{j+\sigma_j} = p^{j+\sigma}\delta_x^2\xi_i^{j+\sigma_j} + {}_cR_i^{j+\sigma},$$

$$1 \leq i \leq N_x - 1, \tag{2.48}$$

$$\xi_i^0 = 0, \quad 0 \leq i \leq N_x, \tag{2.49}$$

$$\xi_0^j = 0, \quad \xi_{N_x}^j = 0, \quad 1 \leq j \leq N_t. \tag{2.50}$$

Since $\xi_i^{j+1} \in \mathcal{D}_h^*$, therefore applying Theorem 2.1 for the error equation (2.48)-(2.50) we have

$$\|\xi^{j+1}\|^2 \leq \tilde{C} \max_{0\leq l\leq N_t-1} \|{}_cR^{l+\sigma}\|^2, \quad 0 \leq j \leq N_t - 1, \tag{2.51}$$

where $\tilde{C} = \frac{12(z(T)-z(0))^\alpha\Gamma(1-\alpha)}{5\epsilon}$ and $\epsilon = \frac{8p^{j+\sigma}}{3b}$.

Since we have the following truncation error bound

$$\max_{0\leq l\leq N_t-1} \|{}_cR^{l+\sigma}\| = \mathcal{O}(\Delta t^{3-\alpha}, \widetilde{\Delta} t^2, h^4),$$

therefore, using it in equation (2.51) yields the theorem. □

2.2.2 Stability and convergence analysis of PQS$_{g-\sigma}$ scheme

In this subsection, we provide stability and convergence analysis of PQS$_{g-\sigma}$ scheme (2.30)-(2.32). We shall use the following lemmas.

Lemma 2.7. *[65] Let $\vartheta \in \mathcal{D}_h^*$. If $\mu \in \left(0, \frac{67}{492}\right)$, then*

$$\Upsilon^2(\vartheta, \vartheta) \leq (\mathcal{H}_q\vartheta, \mathcal{H}_q\vartheta) \leq \left(\frac{61}{60}\right)^2 (\vartheta, \vartheta),$$

where $\Upsilon > 0$ is given by

$$\Upsilon = \begin{cases} -\frac{71\mu}{24} + \frac{283}{480}, & 0 < \mu \leq \frac{1}{20}, \\ -\frac{9\mu}{2} + \frac{2}{3}, & \mu = \frac{1}{20}, \\ -\frac{41\mu}{8} + \frac{67}{96}, & \frac{1}{20} < \mu < \frac{67}{492}. \end{cases}$$

Lemma 2.8. *[65] Let $\vartheta \in \mathcal{D}_h^*$. If $\mu \in (0, \tilde{\mu}_0)$, where $\tilde{\mu}_0 = \frac{-161+12\sqrt{229}}{340}$, then*

$$(\mathcal{H}_q\vartheta, \tilde{\delta}_x^2\vartheta) \leq -\frac{4\Upsilon_1}{b}(\vartheta, \vartheta),$$

where $\Upsilon_1 > 0$ is given by

$$\Upsilon_1 = \begin{cases} \frac{71}{120} - 7\mu + 18\mu^2, & 0 < \mu < \tilde{\mu}_1, \\ \frac{2}{3} - 10\mu, & \mu = \tilde{\mu}_1, \\ \frac{83}{120} - 11\mu - 6\mu^2, & \tilde{\mu}_1 < \mu \leq \frac{1}{20}, \\ \frac{83}{120} - \frac{1288\mu}{120} - \frac{1360\mu^2}{120}, & \frac{1}{20} < \mu < \tilde{\mu}_0. \end{cases}$$

Here, $\tilde{\mu}_0 = \frac{-161+12\sqrt{229}}{340}$ and $\tilde{\mu}_1 = \frac{-5+2\sqrt{10}}{60}$.

Let $\tilde{u}_i^j$ solve the following problem

$$\nu\mathcal{H}_q\left[w_0\tilde{u}_i^{j+1} - \sum_{k=1}^{j}(w_{j-k} - w_{j-k+1})\tilde{u}_i^k - w_j\tilde{u}_i^0\right] + q^{j+\sigma}\mathcal{H}_q\tilde{u}_i^{j+\sigma_j} = p^{j+\sigma}\tilde{\delta}_x^2\tilde{u}_i^{j+\sigma_j}$$
$$+ \mathcal{H}_q\hat{F}_i^{j+\sigma}, \quad 1 \leq i \leq N_x - 1, \qquad (2.52)$$

$$\tilde{u}_i^0 = \hat{g}(x_i), \quad 0 \le i \le N_x, \tag{2.53}$$

$$\tilde{u}_0^j = \phi_1(t_j), \quad \tilde{u}_{N_x}^j = \phi_2(t_j), \quad 1 \le j \le N_t. \tag{2.54}$$

Now, let $e_i^j = \tilde{u}_i^j - U_i^j$. Then from equations (2.30)-(2.32) and (2.52)-(2.54) it is evident that $e_i^j \in \mathcal{D}_h^*$ and solves the following linear system

$$\nu \mathcal{H}_q \left[w_0 e_i^{j+1} - \sum_{k=1}^{j} (w_{j-k} - w_{j-k+1}) e_i^k - w_j e_i^0 \right] + q^{j+\sigma} \mathcal{H}_q e_i^{j+\sigma_j} = p^{j+\sigma} \tilde{\delta}_x^2 e_i^{j+\sigma_j}$$
$$+ \mathcal{H}_q \tilde{F}_i^{j+\sigma}, \quad 1 \le i \le N_x - 1, \tag{2.55}$$

$$e_i^0 = \hat{g}(x_i) - g(x_i), \quad 0 \le i \le N_x, \tag{2.56}$$

$$e_0^j = 0, \quad e_{N_x}^j = 0, \quad 1 \le j \le N_t, \tag{2.57}$$

where $\tilde{F}_i^{j+\sigma} = \hat{F}_i^{j+\sigma} - F_i^{j+\sigma}$. Now we will prove a result that will directly show the stability of the scheme.

Theorem 2.3. *Suppose the inverse of the scale function z is concave. If $\mu \in (0, \tilde{\mu}_0)$, then the solution of the discrete problem (2.55)-(2.57) satisfies*

$$\|e^{j+1}\|^2 \le c \left[\|\mathcal{H}_q e^0\|^2 + \frac{\Gamma(1-\alpha)(z(T) - z(0))^\alpha}{\tilde{\epsilon}} \max_{0 \le l \le N_t - 1} \|\mathcal{H}_q \tilde{F}^{l+\sigma}\|^2 \right], \tag{2.58}$$

where $c = \frac{1}{\Upsilon^2}$ and $\tilde{\epsilon} = \left(\frac{60}{61}\right)^2 \frac{4\Upsilon_1 p^{j+\sigma}}{b} > 0$.

Proof. Multiplying equation (2.55) with $h\mathcal{H}_q e_i^{j+\sigma_j}$ and then summing from $i = 1$ to $N_x - 1$, we get

$$\nu \left[w_0 (\mathcal{H}_q e^{j+\sigma_j}, \mathcal{H}_q e^{j+1}) - \sum_{k=1}^{j} (w_{j-k} - w_{j-k+1}) (\mathcal{H}_q e^{j+\sigma_j}, \mathcal{H}_q e^k) - w_j (\mathcal{H}_q e^{j+\sigma_j}, \mathcal{H}_q e^0) \right]$$
$$= p^{j+\sigma} (\mathcal{H}_q e^{j+\sigma_j}, \tilde{\delta}_x^2 e^{j+\sigma_j}) - q^{j+\sigma} (\mathcal{H}_q e^{j+\sigma_j}, \mathcal{H}_q e^{j+\sigma_j}) + (\mathcal{H}_q e^{j+\sigma_j}, \mathcal{H}_q \hat{F}^{j+\sigma}), \tag{2.59}$$

Next, applying Lemma 2.6 to the left side of the above equation gives

$$w_0(\mathcal{H}_q e^{j+\sigma_j}, \mathcal{H}_q e^{j+1}) - \sum_{k=1}^{j}(w_{j-k} - w_{j-k+1})(\mathcal{H}_q e^{j+\sigma_j}, \mathcal{H}_q e^{k}) - w_j(He^{j+\sigma_j}, \mathcal{H}_q e^0)$$
$$\geq \frac{1}{2}\left[w_0\|\mathcal{H}_q e^{j+1}\|^2 - \sum_{k=1}^{j}(w_{j-k} - w_{j-k+1})\|\mathcal{H}_q e^k\|^2 - w_j\|\mathcal{H}_q e^0\|^2\right]. \tag{2.60}$$

Since $e^j \in \mathcal{D}_h^*$, using Lemma 2.8 to the term $(\mathcal{H}_q e^{j+\sigma_j}, \tilde{\delta}_x^2 e^{j+\sigma_j})$, we have

$$(\mathcal{H}_q e^{j+\sigma_j}, \tilde{\delta}_x^2 e^{j+\sigma_j}) \leq -\frac{4\Upsilon_1}{b}(e^{j+\sigma_j}, e^{j+\sigma_j}). \tag{2.61}$$

Moreover, for any $\tilde{\epsilon} > 0$, applying the Young's inequality and Lemma 2.7 to the term $(\mathcal{H}_q e^{j+\sigma_j}, \mathcal{H}_q \hat{F}^{j+\sigma})$ yields

$$(\mathcal{H}_q e^{j+\sigma_j}, \mathcal{H}_q \hat{F}^{j+\sigma}) \leq \tilde{\epsilon}\|\mathcal{H}_q e^{j+\sigma_j}\|^2 + \frac{1}{4\tilde{\epsilon}}\|\mathcal{H}_q \tilde{F}^{j+\sigma}\|^2 \leq \tilde{\epsilon}\left(\frac{61}{60}\right)^2\|e^{j+\sigma_j}\|^2$$
$$+ \frac{1}{4\tilde{\epsilon}}\|\mathcal{H}_q \tilde{F}^{j+\sigma}\|^2. \tag{2.62}$$

Now, setting $\tilde{\epsilon} = \left(\frac{60}{61}\right)^2 \frac{4\Upsilon_1 p^{j+\sigma}}{b} > 0$ and using inequalities (2.60), (2.61) and (2.62) in equation (2.59) yields

$$w_0\|\mathcal{H}_q e^{j+1}\|^2 - \sum_{k=1}^{j}(w_{j-k} - w_{j-k+1})\|\mathcal{H}_q e^k\|^2 - w_j\|\mathcal{H}_q e^0\|^2 \leq \frac{b}{8\nu\Upsilon_1 p^{j+\sigma}}\left(\frac{61}{60}\right)^2$$
$$\|\mathcal{H}_q \tilde{F}^{j+\sigma}\|^2,$$

hence,

$$w_0\|\mathcal{H}_q e^{j+1}\|^2 - \sum_{k=1}^{j}(w_{j-k} - w_{j-k+1})\|\mathcal{H}_q e^k\|^2 \leq w_j\left[\|\mathcal{H}_q e^0\|^2 + \frac{b}{8\nu\Upsilon_1 p^{j+\sigma} w_j}\left(\frac{61}{60}\right)^2\right.$$
$$\left.\times\|\mathcal{H}_q \tilde{F}^{j+\sigma}\|^2\right].$$

Thus, using Lemma 2.1 and noting that $(j+\sigma)\Delta t = \frac{(j+\sigma)(z(T)-z(0))}{N_t} < (z(T)-z(0))$, we get

$$w_0\|\mathcal{H}_q e^{j+1}\|^2 - \sum_{k=1}^{j}(w_{j-k}-w_{j-k+1})\|\mathcal{H}_q e^k\|^2 \leq w_j\widetilde{\chi}, \tag{2.63}$$

where

$$\widetilde{\chi} = \|\mathcal{H}_q e^0\|^2 + \frac{\Gamma(1-\alpha)(z(T)-z(0))^\alpha}{\tilde{\epsilon}} \max_{0\leq l\leq N_t-1} \|\mathcal{H}_q \tilde{F}^{l+\sigma}\|^2.$$

Now, we proceed as in Theorem 2.1 and can prove by induction that

$$\|\mathcal{H}_q e^{j+1}\|^2 \leq \widetilde{\chi}, \quad 0 \leq j \leq N_t - 1. \tag{2.64}$$

Further, using Lemma 2.7 in (2.64) gives (2.58). $\square$

In view of equation (2.5), Lemmas 2.3 and 2.4, we have

$${}_qR_i^{j+\sigma} = \begin{cases} \mathcal{O}(\Delta t^{3-\alpha}, \widetilde{\Delta} t^2, h^4), & i = 1, N_x - 1, \\ \mathcal{O}(\Delta t^{3-\alpha}, \widetilde{\Delta} t^2, h^6), & 2 \leq i \leq N_x - 2. \end{cases} \tag{2.65}$$

Now we will prove the main convergence theorem.

Theorem 2.4. *Let $u(x,t) \in C^{8,2}([0,b]\times[0,T])$ be the solution of problem (2.3)-(2.4), $u(x,\mathcal{Z}^{-1}(z)) \in C^3[z(T)-z(0)]$ for any fixed x, inverse of z is concave, and $\{U_i^j, 0 \leq i \leq N_x, 1 \leq j \leq N_t\}$ be the solution of the discrete problem (2.30)-(2.32). Then the following result holds*

$$\|u_i^{j+1} - U_i^{j+1}\| \leq c\ \mathcal{O}\left(\Delta t^{3-\alpha}, \widetilde{\Delta} t^2, h^{4.5}\right), \tag{2.66}$$

where $c = \sqrt{\frac{\widetilde{m}(z(T)-z(0))^\alpha\Gamma(1-\alpha)}{\tilde{\epsilon}\Upsilon^2}}$, $\tilde{\epsilon} = \frac{8p^{j+\sigma}}{3b}$, and $\widetilde{m}$ is a postive constant independent of h, Δt, and $\widetilde{\Delta} t$.

***Proof*.** Let $\xi_i^{j+1} = u_i^{j+1} - U_i^{j+1}$. Now subtracting the linear system (2.30)-(2.32) from (2.27)-(2.29) we get

$$\nu\mathcal{H}_q\left[w_0\xi_i^{j+1} - \sum_{k=1}^{j}(w_{j-k} - w_{j-k+1})\xi_i^k - w_j\xi_i^0\right] + q^{j+\sigma}\mathcal{H}_q\xi_i^{j+\sigma_j} = p^{j+\sigma}\tilde{\delta}_x^2\xi_i^{j+\sigma_j} + {}_qR_i^{j+\sigma},$$

$$1 \le i \le N_x - 1, \tag{2.67}$$

$$\xi_i^0 = 0, \quad 0 \le i \le N_x, \tag{2.68}$$

$$\xi_0^j = 0, \quad \xi_{N_x}^j = 0, \quad 1 \le j \le N_t. \tag{2.69}$$

Since $\xi_i^{j+1} \in \mathcal{D}_h^*$, therefore applying Theorem 2.3 to the error equation (2.67)-(2.69) we have

$$\|\xi^{j+1}\|^2 \le \hat{C} \max_{0\le l\le N_t-1} \|{}_qR^{l+\sigma}\|^2, \quad 0 \le j \le N_t - 1, \tag{2.70}$$

where $\hat{C} = \frac{\Gamma(1-\alpha)(z(T)-z(0))^\alpha}{\tilde{\epsilon}\Upsilon^2}$ and $\tilde{\epsilon} = \left(\frac{61}{60}\right)^2 \frac{4\Upsilon_1 p^{j+\sigma}}{b}$.

Thus, we are left to bound $\|{}_qR^{l+\sigma}\|^2$ in equation (2.70). Using equation (2.65), and noting $(N_x - 3)h \le b$, we proceed as follows

$$\begin{aligned}
\|{}_qR^{l+\sigma}\|^2 =& h\sum_{i=1}^{N_x-1}\left(R^{l+\sigma}\right)^2 \\
=& 2h\left(\mathcal{O}(\Delta t^{3-\alpha}, \widetilde{\Delta} t^2, h^4)\right)^2 + h(N_x - 3)\left(\mathcal{O}(\Delta t^{3-\alpha}, \widetilde{\Delta} t^2, h^6)\right)^2 \\
\le& 2\left(\mathcal{O}(\Delta t^{3-\alpha}, \widetilde{\Delta} t^2, h^{4.5})\right)^2 + b\left(\mathcal{O}(\Delta t^{3-\alpha}, \widetilde{\Delta} t^2, h^6)\right)^2 \\
\le& \widetilde{m}\left(\mathcal{O}(\Delta t^{3-\alpha}, \widetilde{\Delta} t^2, h^{4.5})\right)^2,
\end{aligned}$$

where $\widetilde{m}$ is a positive constant, which is independent of l and h.

Substituting the above result into equation (2.70) leads to (2.66) immediately. Thus, the proof is complete. □

2.3 Numerical results

In this segment, we present results for three numerical examples to assess the practical performance of the proposed numerical schemes. If $v(x_i, t_j)$ and $V(x_i, t_j)$ are the exact and approximate solutions of problem (2.1)-(2.2) respectively at (x_i, t_j), then the accuracy of the numerical solution will be measured as follows

$$\mathcal{L}_\infty(h, \Delta t) = \|v - V\|_\infty = \max_{1\le j\le N_t} \max_{1\le i\le N_x} |v(x_i, t_j) - V(x_i, t_j)|, \tag{2.71}$$

$$\mathcal{L}_2(h, \Delta t) = \|v - V\|_2 = \max_{1\le j\le N_t} \sqrt{h \sum_{i=1}^{N_x - 1} (v(x_i, t_j) - V(x_i, t_j))^2}. \tag{2.72}$$

We evaluate the order of convergence as follows

$$cov.order = \begin{cases} log_2 \left(\frac{\mathcal{L}_l(h,\Delta t_1)}{\mathcal{L}_l(h,\Delta t_2)}\right), & \text{in time,} \\ log_2 \left(\frac{\mathcal{L}_l(h_1,\Delta t)}{\mathcal{L}_l(h_2,\Delta t)}\right), & \text{in space,} \end{cases} \tag{2.73}$$

where $l = 2$ or ∞.

Example 2.1. [68, 119] Let us consider problem (2.1)-(2.2) on the domain $(0, 1) \times (0, 1]$ with the assumption that the function $v(x, t) = \sin(\pi x) + x(x - 1)z(t)^2$ is the exact solution.

We have solved this problem taking different $z(t)$, $\omega(t)$, $p(t)$, and $q(t)$ functions, and display the results in Tables 2.1, 2.2, 2.3, and 2.4. $\mathcal{L}_2$-error and corresponding spatial orders of convergence for both schemes $\text{CFD}_{g-\sigma}$ and $\text{PQS}_{g-\sigma}$ are given in Table 2.1 with scale function $z(t) = e^{2t} - 1$, weight function $\omega(t) = e^t$, $q(t) = 1 - \sin t$ and $p(t) = t$. From this table, we observe that the spatial orders of convergence for $\text{CFD}_{g-\sigma}$ and $\text{PQS}_{g-\sigma}$ schemes are almost 4 and at least 4.5 respectively, which are consistent with our theoretical findings. These are the highest spatial order of

TABLE 2.1: (Example 2.1) $\mathcal{L}_2$-error and spatial orders of convergence taking $N_t = 7000$, $z(t) = e^{2t} - 1$ and $\omega(t) = e^t$.

		$\text{CFD}_{g-\sigma}$		$\text{PQS}_{g-\sigma}$	
α	N_x	$\mathcal{L}_2$-error	cov.order$_x$	$\mathcal{L}_2$-error	cov.order$_x$
0.2	2^2	4.8023e-04	-	2.2043e-04	-
	2^3	3.3416e-05	3.8451	2.5701e-06	6.4224
	2^4	2.1241e-06	3.9756	3.6534e-08	6.1364
0.5	2^2	4.9622e-04	-	2.2816e-04	-
	2^3	3.4539e-05	3.8447	2.6623e-06	6.4212
	2^4	2.2080e-06	3.9674	5.0752e-08	5.7131
0.8	2^2	5.2026e-04	-	2.3959e-04	-
	2^3	3.6218e-05	3.8444	2.7936e-06	6.4223
	2^4	2.3223e-06	3.9631	6.0568e-08	5.5274

convergence in comparison to the existing works for solving generalized fractional reaction-diffusion equation (2.1)-(2.2). Moreover, in Tables 2.2 and 2.3, we have compared the proposed work with the existing works [68, 119] taking $q(t) = 0$, $p(t) = 1$ and different scale and weight functions. Table 2.2 shows that the temporal order of convergence of proposed schemes is two, which is higher than $2 - \alpha$ [119], where α is the fractional order. Further, from Table 2.3, it is clear that $\text{CFD}_{g-\sigma}$ and $\text{PQS}_{g-\sigma}$ schemes give very small errors, but in the case of the $\text{PQS}_{g-\sigma}$ scheme the convergence order is not as expected - this is because the temporal mesh width not being sufficiently small. Whereas in Table 2.4, taking $N_t = 20000$, we observe that the convergence order for the $\text{PQS}_{g-\sigma}$ scheme is at least 4.5, which is consistent with Theorem 2.4.

Furthermore, Figure 2.1 represents the absolute error plots for Example 2.1 obtained using the $\text{CFD}_{g-\sigma}$ and $\text{PQS}_{g-\sigma}$ schemes taking $z(t) = e^{2t} - 1$, $\omega(t) = e^t$, $p(t) = t$, and $q(t) = 1 - \sin t$. This figure indicates that both proposed schemes approximate the problem well.

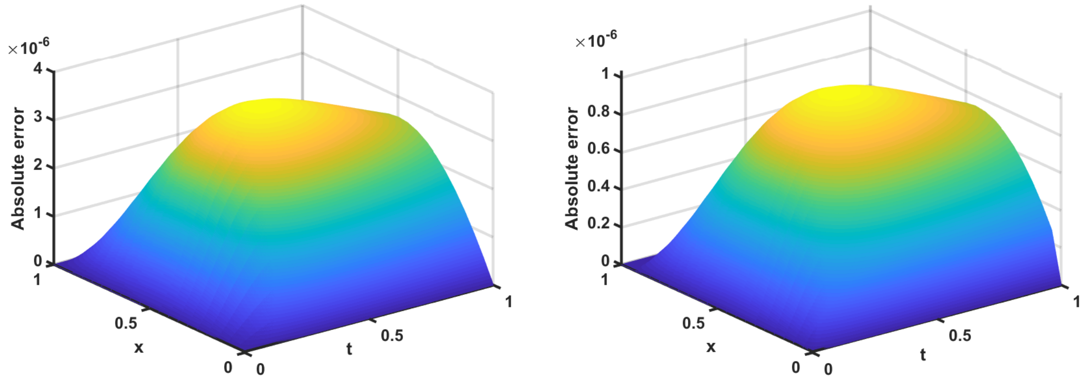

(a) CFD$_{g-\sigma}$ (b) PQS$_{g-\sigma}$

FIGURE 2.1: $\mathcal{L}_\infty\left(\frac{1}{20}, \frac{1}{1000}\right)$ with $\alpha = 0.8$ for Example 2.1.

TABLE 2.2: (Example 2.1) Comparison with method in [119] taking $\alpha = 0.85$ and $N_x = 1000$.

		[119]		CFD$_{g-\sigma}$		PQS$_{g-\sigma}$	
	N_t	$\mathcal{L}_\infty$-error	cov.order$_t$	$\mathcal{L}_\infty$-error	cov.order$_t$	$\mathcal{L}_\infty$-error	cov.order$_t$
$z(t) = t$,	50	2.25e-04	-	2.3953e-05	-	2.3953e-05	-
$\omega(t) = 1$	100	9.72e-05	1.21	5.9883e-06	2.00	5.9883e-06	2.00
	200	3.98e-05	1.29	1.4971e-06	2.00	1.4971e-06	2.00
$z(t) = t$,	50	2.56e-04	-	1.7357e-05	-	1.7357e-05	-
$\omega(t) = e^t$	100	1.12e-04	1.19	4.3385e-06	2.00	4.3385e-06	2.00
	200	4.62e-05	1.28	1.0849e-06	1.99	1.0849e-06	1.99

Example 2.2. [67] Let us consider problem (2.3)-(2.4) on the domain $(0, 1) \times (0, 1]$ with the assumption that the function $u(x, t) = e^x z(t)^\delta$ is the exact solution.

We have solved this problem taking $\delta = 3$ and different $p(t)$, $q(t)$, and scale functions $z(t)$ and display the results in Tables 2.5, 2.6, 2.7 and 2.8. In Tables 2.5 and 2.6, we have taken $p(t) = \sin t$, $q(t) = \cos t$. Further, in Table 2.5, we have taken $z(t) = \cos(0.1) - \cos(\varrho t + 0.1)$ and show that the temporal order of convergence for different fractional order obtained using CFD$_{g-\sigma}$ scheme is almost 2, which is same as the theoretical order. Similarly, Table 2.6 display the temporal order of convergence obtained using PQS$_{g-\sigma}$ scheme taking $z(t) = e^{\varrho t} - 1$. Moreover, for Tables 2.7 and

TABLE 2.3: (Example 2.1) Comparison with method in [68] taking $z(t) = t^2$, $\omega(t) = 1$ and $N_t = 2000$.

		[68]		$\text{CFD}_{g-\sigma}$		$\text{PQS}_{g-\sigma}$	
α	N_x	$\mathcal{L}_2$-error	cov.order$_x$	$\mathcal{L}_2$-error	cov.order$_x$	$\mathcal{L}_2$-error	cov.order$_x$
0.2	10	5.2701e-3	-	2.6242e-05	-	1.0994e-06	-
	20	1.3131e-3	2.00	1.6544e-06	3.98	1.6088e-08	6.09
	40	3.2791e-4	2.00	1.0874e-07	3.92	5.7686e-09	1.47
0.5	10	5.4177e-3	-	3.8445e-05	-	1.1328e-06	-
	20	1.3497e-3	2.01	2.4113e-06	3.99	2.2719e-08	5.63
	40	3.3704e-4	2.00	1.5556e-07	3.95	1.2212e-08	0.89
0.8	10	5.6052e-3	-	3.9738e-05	-	1.1729e-06	-
	20	1.3961e-3	2.01	2.4969e-06	3.99	2.6947e-08	5.44
	40	3.4862e-4	2.00	1.6044e-07	3.96	1.6123e-08	0.74

TABLE 2.4: (Example 2.1) $\mathcal{L}_2$-error and spatial order of convergence taking $z(t) = t^2$, $\omega(t) = 1$, $q(t) = 0$, $p(t) = 1$, and $N_t = 20000$ using $\text{PQS}_{g-\sigma}$ scheme.

	$\alpha = 0.2$		$\alpha = 0.5$		$\alpha = 0.8$	
N_x	$\mathcal{L}_2$-error	cov.order$_x$	$\mathcal{L}_2$-error	cov.order$_x$	$\mathcal{L}_2$-error	cov.order$_x$
10	1.1583e-06	-	1.1856e-06	-	1.2218e-06	-
20	1.0822e-08	6.7420	1.1137e-08	6.7341	1.1512e-08	6.7297
40	1.6282e-10	6.0545	2.2935e-10	5.6016	2.7175e-10	5.4047

2.8 we have taken $p(t) = 1$, $q(t) = 0$. Table 2.7 compares the $\mathcal{L}_2$-error and spatial orders of convergence obtained using $\text{CFD}_{g-\sigma}$ and $\text{PQS}_{g-\sigma}$ schemes with the central difference scheme in [67], taking $z(t) = \cos(0.1) - \cos(\varrho t + 0.1)$. From this table, we observe that the spatial orders of convergence of $\text{CFD}_{g-\sigma}$ and $\text{PQS}_{g-\sigma}$ scheme are 4 and 4.5, respectively, which are higher than two, in [67]. Further, Table 2.8 compares the same results as Table 2.7 with different scale function $z(t) = e^{\varrho t} - 1$.

Just like Figure 2.1, we plot the absolute errors in Figure 2.3 for Example 2.2 obtained using the $\text{CFD}_{g-\sigma}$ and $\text{PQS}_{g-\sigma}$ schemes taking $z(t) = \cos(0.1) - \cos(1.1t + 0.1)$, $p(t) = \sin t$, and $q(t) = \cos t$. Obviously, this figure indicates that we get a good

TABLE 2.5: (Example 2.2) $\mathcal{L}_2$-error and spatial orders of convergence with $h = \frac{1}{500}$ and $z(t) = \cos(0.1) - \cos(\varrho t + 0.1)$ using $\text{CFD}_{g-\sigma}$ scheme.

α	ϱ	N_t	$\mathcal{L}_2$-error	cov.order$_t$	ϱ	$\mathcal{L}_2$-error	cov.order$_t$
0.2	1.1	40	1.9014e-06	-	0.9	7.2140e-07	-
		80	4.9686e-07	1.9362		1.8888e-07	1.9334
		160	1.2761e-07	1.9610		4.8565e-08	1.9594
0.5		40	4.2947e-06	-		1.6137e-06	-
		80	9.8953e-07	2.1177		3.6807e-07	2.1324
		160	2.2997e-07	2.1053		8.4707e-08	2.1194
0.8		40	9.1887e-06	-		3.7050e-06	-
		80	2.1362e-06	2.1048		8.5381e-07	2.1175
		160	4.9573e-07	2.1074		1.9642e-07	2.1200

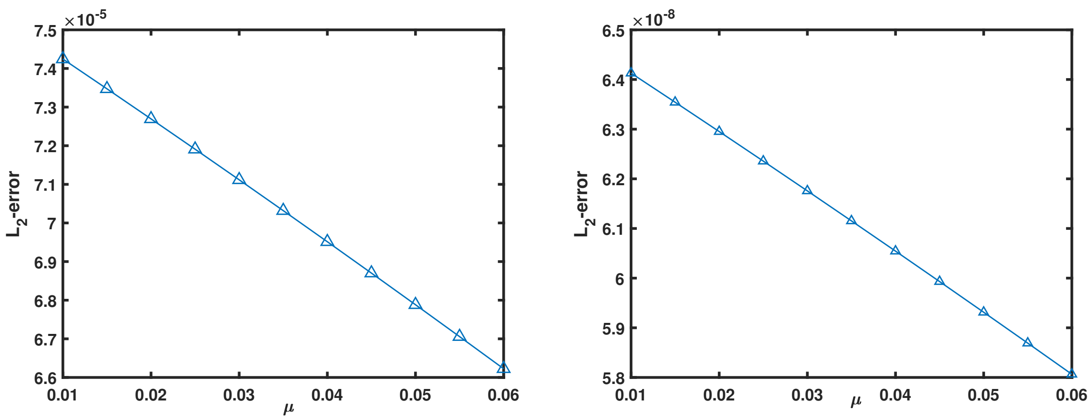

(a) Example 2.1 (b) Example 2.2

FIGURE 2.2: $\mathcal{L}_2\left(\frac{1}{5}, \frac{1}{1000}\right)$ for various μ with $\alpha = 0.5$.

approximation. Finally, we examine how alpha affects the errors obtained using the $\text{PQS}_{g-\sigma}$ scheme. Therefore, in Figure 2.2 we plot the $\mathcal{L}_2$-error for different values of $\mu \in (0, \tilde{\mu}_0)$ and observe that this has little effect on the errors. Therefore, the choice of μ can be any in $(0, \tilde{\mu}_0)$.

TABLE 2.6: (Example 2.2) $\mathcal{L}_2$-error and temporal order of convergence with $h = \frac{1}{500}$ and $z(t) = e^{\varrho t} - 1$ using PQS$_{g-\sigma}$ scheme.

α	ϱ	N_t	$\mathcal{L}_2$-error	cov.order$_t$	ϱ	$\mathcal{L}_2$-error	cov.order$_t$
0.2	1.1	40	7.5880e-05	-	0.9	2.7976e-05	-
		80	1.9577e-05	1.9546		7.2383e-06	1.9505
		160	4.9885e-06	1.9725		1.8476e-06	1.9700
0.5		40	1.5993e-04	-		6.5261e-05	-
		80	3.8269e-05	2.0632		1.5527e-05	2.0715
		160	9.5408e-06	2.0040		3.7120e-06	2.0645
0.8		40	2.7154e-04	-		1.1513e-04	-
		80	6.5156e-05	2.0592		2.7432e-05	2.0693
		160	1.5623e-05	2.0602		6.5349e-06	2.0696

TABLE 2.7: (Example 2.2) Comparison with method in [67] taking $z(t) = \cos(0.1) - \cos(\varrho t + 0.1)$, $\omega(t) = 1$, $\varrho = 1.1$, and $N_t = 20000$.

		[67]		CFD$_{g-\sigma}$		PQS$_{g-\sigma}$	
α	N_x	$\mathcal{L}_2$-error	cov.order$_x$	$\mathcal{L}_2$-error	cov.order$_x$	$\mathcal{L}_2$-error	cov.order$_x$
0.2	5	1.1338e-04	-	2.2775e-07	-	8.5343e-08	-
	10	2.8503e-05	1.9919	1.4241e-08	3.9993	1.4440e-09	5.8851
	20	7.1344e-06	1.9983	8.6531e-10	4.0407	1.2439e-11	6.8590
0.5	5	1.0479e-04	-	2.2775e-07	-	7.9537e-08	-
	10	2.6390e-05	1.9894	1.3163e-08	4.0023	1.3294e-09	5.9028
	20	6.6083e-06	1.9976	7.7203e-10	4.0917	3.5806e-11	5.2144
0.8	5	9.3182e-05	-	1.8815e-07	-	7.1735e-08	-
	10	2.3526e-05	1.9858	1.1728e-08	4.0039	1.2016e-09	5.8997
	20	5.8947e-06	1.9968	6.7337e-10	4.1224	4.7039e-11	4.6749

TABLE 2.8: (Example 2.2) Comparison with method in [67] taking $z(t) = e^{\varrho t} - 1$, $\omega(t) = 1$, $\varrho = 0.9$, and $N_t = 20000$.

		[67]		$\text{CFD}_{g-\sigma}$		$\text{PQS}_{g-\sigma}$	
α	N_x	$\mathcal{L}_2$-error	cov.order$_x$	$\mathcal{L}_2$-error	cov.order$_x$	$\mathcal{L}_2$-error	cov.order$_x$
0.2	5	1.4202e-03	-	2.8513e-06	-	1.0668e-06	-
	10	3.5689e-04	1.9926	1.7824e-07	3.9997	1.7976e-08	5.8911
	20	8.9322e-05	1.9984	1.0787e-08	4.0465	1.7241e-10	6.7041
0.5	5	1.3788e-03	-	2.7702e-06	-	1.0386e-06	-
	10	3.4673e-04	1.9916	1.7278e-07	4.0030	1.7165e-08	5.9190
	20	8.6792e-05	1.9982	1.0057e-08	4.1026	5.4647e-10	4.9732
0.8	5	1.3328e-03	-	2.6803e-06	-	1.0075e-06	-
	10	3.3543e-04	1.9904	1.6696e-07	4.0048	1.6506e-08	5.9316
	20	8.3980e-05	1.9979	9.5043e-09	4.1348	7.5257e-10	4.4550

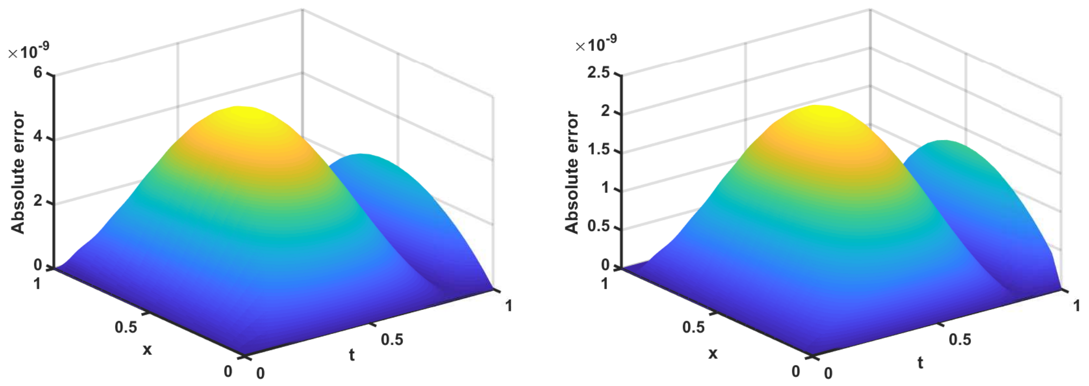

(*a*) $\text{CFD}_{g-\sigma}$ (*b*) $\text{PQS}_{g-\sigma}$

FIGURE 2.3: $\mathcal{L}_\infty\left(\frac{1}{20}, \frac{1}{1000}\right)$ with $\alpha = 0.6$ for Example 2.2.

Example 2.3. [66, 119] Let us consider problem (2.1)-(2.2) on the domain $(0,1) \times (0,1]$. We will solve this problem taking $\hat{\phi}_1(t) = \hat{\phi}_2(t) = 0$, $g_0(x) = x(1-x)^3 \exp(\sin 3.5\pi x)$, $q(t) = 0$, and source function $\mathscr{F}(x,t) = \frac{(x-1)(t-1)}{2+\sin xt}$.

In this problem, we will provide a few plots to examine the effect of the scale function $z(t)$, the weight function $\omega(t)$, and the diffusion function $p(t)$ on the solution obtained using the $\text{CFD}_{g-\sigma}$ scheme. So, we have fixed the values $\alpha = 0.92$, $N_x = 150$, and $N_t = 1000$ to make a fair comparison in all cases.

In Figure 2.4, we plot the three-dimensional graphics of the discrete solutions under the four cases as follows.

1. $\omega(t) = e^t$, $z(t) = t$, and $p(t) = 1.2$; (base case).
2. $\omega(t) = e^t$, $z(t) = t^6$, and $p(t) = 1.2$; (change $z(t)$).
3. $\omega(t) = e^{6t}$, $z(t) = t$, and $p(t) = 1.2$; (change $\omega(t)$).
4. $\omega(t) = e^t$, $z(t) = t$, and $p(t) = 0.6$; (change $p(t)$).

The following comments have been noted:

- From Figure 2.4(a), we note that eventually, the numerical solution tends to zero as we have taken the zero boundary conditions.
- From Figure 2.4(b), we see that as the scale function is contracted, the stretching of the time domain takes place near $t = 0$, which provides a coarser mesh compared to Figure 2.4(a).
- In Figure 2.4(c), we have taken a larger weight function $\omega(t) = e^{6t}$ as compared to Figure 2.4(a), which shows the solution has become smaller. Furthermore, we see from this figure that since the weight function is monotonically increasing, this makes the diffusion phenomenon fast.
- In Figure 2.4(d), we have assumed a smaller value of diffusion function ($p(t) = 0.6$) than in Figure 2.4(a) ($p(t) = 1.2$); consequently, the diffusion process slows down in this case.

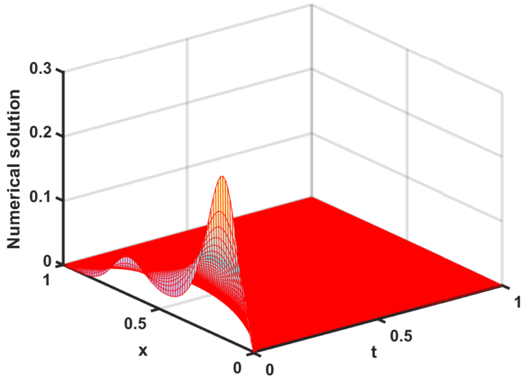

Case 1. $\omega(t) = e^t$, $z(t) = t$, and $p(t) = 1.2$

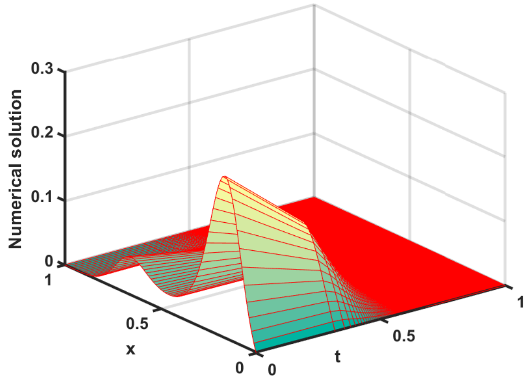

Case 2. $\omega(t) = e^t$, $z(t) = t^6$, and $p(t) = 1.2$

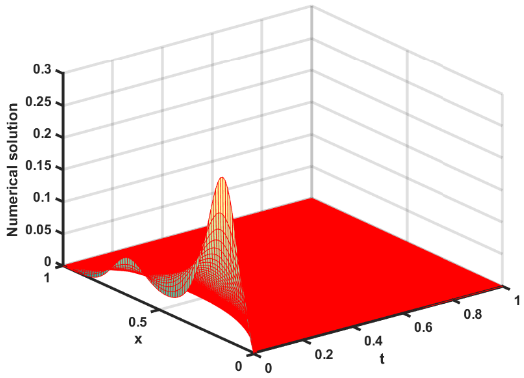

Case 3. $\omega(t) = e^{6t}$, $z(t) = t$, and $p(t) = 1.2$

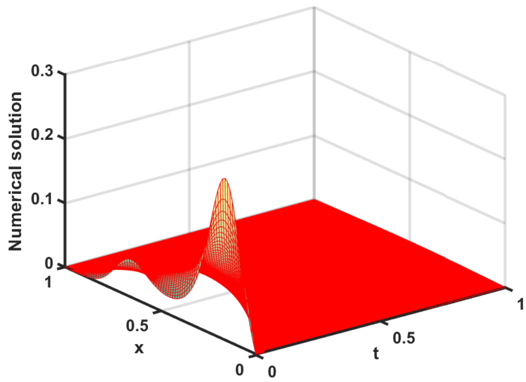

Case 4. $\omega(t) = e^t$, $z(t) = t$, and $p(t) = 0.6$

FIGURE 2.4: Numerical solutions of Example 2.3.

2.4 Conclusion

In this chapter, two high-order schemes, $\text{CFD}_{g-\sigma}$ and $\text{PQS}_{g-\sigma}$, have been developed for the variable coefficients generalized fractional reaction-diffusion equation. The $\text{CFD}_{g-\sigma}$ scheme combined the $gL2-1_\sigma$ approximation of fractional time derivative with a compact space difference scheme, whereas the $\text{PQS}_{g-\sigma}$ scheme has been formulated using the $gL2-1_\sigma$ formula for temporal discretization along with the parametric quintic splines for spatial discretization. The theoretical analysis, which included the stability and convergence of both schemes, has been rigorously established using the discrete energy method in $\mathcal{L}_2$-norm. The convergence orders $\mathcal{O}(\Delta t^{3-\alpha}, \widetilde{\Delta} t^2, h^4)$ and $\mathcal{O}(\Delta t^{3-\alpha}, \widetilde{\Delta} t^2, h^{4.5})$ of $\text{CFD}_{g-\sigma}$ and $\text{PQS}_{g-\sigma}$ schemes, respectively, have improved the existing works and are best till date for the variable coefficients generalized fractional reaction-diffusion equation. Finally, numerical experiments have been performed to show the accuracy and efficiency of the proposed schemes.